

UNIVERSIDAD SAN FRANCISCO DE QUITO USFQ

Colegio de Ciencias e Ingenierías

**Programmable MPPT Solar Charger Controller using
Inverting Buck-Boost power converter.**

Proyecto de Investigación

Bolívar Daniel Alvarez Muñoz
Ingeniería Electronica

Trabajo de titulación presentado como requisito
para la obtención del título de
Ingeniero Electrónico

Quito, 21 de mayo de 2018

UNIVERSIDAD SAN FRANCISCO DE QUITO USFQ
COLEGIO DE CIENCIAS E INGENIERIA

**HOJA DE CALIFICACIÓN
DE TRABAJO DE TITULACIÓN**

Programmable MPPT Solar Charger Controller using
Inverting Buck-Boost power converter.

Bolívar Daniel Alvarez Muñoz

Calificación:

Nombre del profesor, Título académico

Alberto Sánchez , Ph.D.

Firma del profesor

Quito, 21 de mayo de 2018

Derechos de Autor

Por medio del presente documento certifico que he leído todas las Políticas y Manuales de la Universidad San Francisco de Quito USFQ, incluyendo la Política de Propiedad Intelectual USFQ, y estoy de acuerdo con su contenido, por lo que los derechos de propiedad intelectual del presente trabajo quedan sujetos a lo dispuesto en esas Políticas.

Asimismo, autorizo a la USFQ para que realice la digitalización y publicación de este trabajo en el repositorio virtual, de conformidad a lo dispuesto en el Art. 144 de la Ley Orgánica de Educación Superior.

Firma del estudiante: _____

Nombres y apellidos: Bolívar Daniel Alvarez Muñoz

Código: 112763

Cédula de Identidad: 1719468496

Lugar y fecha: Quito, 21 de mayo de 2018

RESUMEN

Este documento informa sobre el diseño y la implementación de un controlador solar de seguimiento de máxima potencia con alta eficiencia para un panel solar de 100W. El proyecto utiliza un microcontrolador Atmel atmega-2560 para ajustar el ciclo de trabajo de dos convertidores inversores Buck-Boost que suministran energía desde el panel solar a una batería paralela y una carga. Para proteger el microcontrolador, de la etapa de alta potencia, es necesario el uso de instrumentos de aislamiento. El algoritmo de Mppt que trabaja con los convertidores inversores Buck-Boost tiene una eficiencia de transferencia de energía del 85% con una carga de 10 Ohms y una batería de descarga.

Palabras clave: Buck-Boost, Punto de Máxima Potencia, MPPT, Micro-controlador Electrónica de Potencia, Instrumentación, aislamiento.

ABSTRACT

This paper reports on the design and implementation of a maximum power point tracker solar charger controller with a high efficiency for a 100W solar panel. The project use an atmel atmega-2560 micro-controller to adjust the duty cycle of two inverter buck-boost converters that supply energy from solar panel to a parallel battery and a load. To protect the micro-controller, from the high power stage, the use of isolation instrumentation is necessary. The Mppt algorithm working with the inverting buck-boost converters has energy transfer efficiency of 85% with a 10 Ohms Load and a discharger Battery.

Key words: Buck-Boost, Maximum Point Power Tracking MPPT, Micro-controller, Power Electronics, Instrumentation, Isolation.

TABLA DE CONTENIDO

Abstract.....	7
Introduction.....	7
Power Stage.....	7
Control Stage.....	10
Results.....	11
Conclutions.....	12
References.....	12

Programmable MPPT Solar Charger Controller using Inverting Buck-Boost power converter.

Bolívar Alvarez, *Student Member, IEEE*, and Alberto Sánchez, *Senior Member, IEEE*

Abstract—This paper reports on the design and implementation of a maximum power point tracker solar charger controller with a high efficiency for a 100W solar panel. The project uses an atmel atmega-2560 micro-controller to adjust the duty cycle of two inverter buck-boost converters that supply energy from solar panel to a parallel battery and a load. In order to protect the micro-controller from the high power stage, the use of isolation instrumentation is necessary. The Mppt algorithm working with the inverting buck-boost converters has energy transfer efficiency of 85% with a 10Ω Load and a discharger Battery.

I. INTRODUCTION

THE use of solar energy is a great deal nowadays, so a efficiency energy management is required[1]. The challenge of manage solar energy is the solar irradiation dependence on different voltages and currents outputs. These variations need to be controlled and stabilized to supply energy to any kind of load. Power electronic is the best way to acquire and process solar energy taking care of minimizing heat losses. There are several commercial products that manage solar energy. Each one has different power electronic topologies and are controlled by intelligent algorithms that try to maximize power supply.

Solar energy is given in DC voltage so the implementation of DC-DC converters is absolutely necessary. There are different topologies of these converters with specific features that manage voltage supplied to the load. Each topology has limitations about the current that can support to the load and even the heat losses that are willing to tolerate. The election and design of the DC-DC converter is fundamental to manage solar energy and is strictly related to the PV and load for which is designed.

DC-DC converters are power electronic circuits that need to be controlled for a properly work[2]. There are two main ways to control the DC-DC converters when working with solar energy. The control can be implemented by a physical circuit which uses comparators and triggers to administrate the duty cycle of the converter. The other alternative is the implementation of a micro-controller. Micro-controllers have a great advantage due to the different and complex algorithms that work with feedback loops and immediately adjust the duty cycle to the best work conditions of the PV. In solar energy management, the Maximum power point tracking (Mppt) algorithm supplies the load with almost all the power that the PV

B. Alvarez is with Universidad San Francisco de Quito USFQ, Colegio de Ciencias e Ingeniería, Campus Cumbayá, PO-Box 17-1200-841, Quito, Ecuador, (email:balvarez@estud.usfq.edu.ec)

A. Sánchez is with Universidad San Francisco de Quito USFQ, Colegio de Ciencias e Ingeniería, Campus Cumbayá, PO-Box 17-1200-841, Quito, Ecuador, (email:asanchez@usfq.edu.ec)

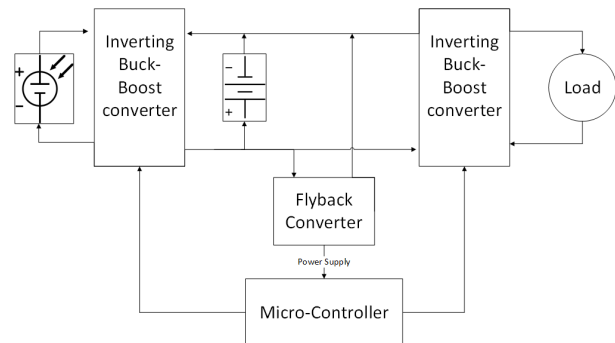


Fig. 1: Block diagram of the power stage

can supply regardless the heat losses and the instrumentation energy consumption. Mppt algorithm works by searching the power point of the PV with a certain solar irradiation. As the solar irradiation keep changing, this algorithm needs of continuous feedback from voltage and current. By implementing feedback loops, the Mppt algorithm guarantees a constant voltage or a constant current required by the load.

In power electronic, it is suitable to isolate the power stage as a DC-DC converter and the control stage as a micro-controller. The isolation of signals give opto-couplers and opto-diodes a great importance since they are low power consumption and linear in properly ranges. For the power supply of the control stage there are two options such as independent batteries or a integrated isolated supply that gives another challenge due to the imminent use of a galvanic isolation devise. There are some topologies of DC-DC converters that give galvanic isolation but need to be carefully design so as to work properly.

The work presented in this paper describes the development of a Mppt solar controller. The paper is organized in the following way. Section II presents a description of the design of the power stage including the galvanic isolated supply for the micro-controller. Section III presents a description of the control stage design. Section IV analyzes the results of the solar charger implementation. Finally, conclusions are drawn in section V.

II. POWER STAGE DESIGN

The power stage design consist of three DC-DC converters. The first two work together to manage the solar energy as described in Figure(1).

The two DC-DC converters have the same topology and similar operation parameters since they work together. The third converter supply energy to the control stage with a galvanic isolation element. The use of a battery is important

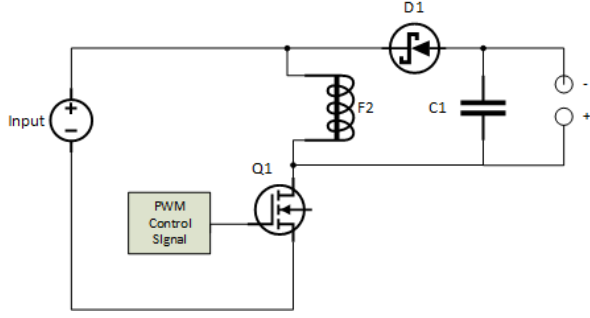


Fig. 2: Inverted Buck-Boost converter

to supply energy to the load in case of low solar irradiation[3] and to ensure that the control stage is always working. The design procedure of the DC-DC converters proposed in this paper is divided into three main circuits.

- 1) DC-DC converters for solar energy management
- 2) DC-DC converter with galvanic isolation
- 3) Active components.

The following subsections present the details of these steps.

A. DC-DC converter for solar energy management

The design of the DC-DC converter is related to the electric features of the PV and the battery. A 100W PV in open circuit gives voltages that fluctuate around 20V depending on solar irradiation[4], whereas a lead battery gives voltages that fluctuate around 12.5V. To charge the battery, the DC-DC converter must adjust the solar voltage to the Float voltage of the battery which in this case is 13.3V. Therefore a Buck converter could perfectly work. However, in low solar irradiation situations the Pv voltage could get lower than 13.3V and still supply current to the load. This means that if the DC-DC converter just reduces the voltage, some solar energy would be dismissed. To avoid that energy dismiss, the topology of the converter must be a buck-boost[[2].

For the project two inverted buck-boost converters[5] as the one shown in Figure(2) were implemented. The first converter goes from PV to Battery. The second converter goes from Battery to the load.

Inverted Buck-Boost converters have the advantage of being manageable with only one duty cycle. Therefore, it is possible to go from Buck mode to Boost mode easily[6] and without signal synchronism problems as in other topologies. This circuit must supply continuous current and a proper voltage ripple. For a continuous current, a proper inductance must be calculated using equation(1)

$$L(\min) = \frac{(1 - D)^2(R)}{2(f)} \quad (1)$$

where D is the duty cycle, R is the load, and f is the switching frequency[5]. The duty cycle is calculated using equation(2).

$$V(\text{out}) = V(\text{in}) \frac{(|D|)}{|(1 - D)|} \quad (2)$$

TABLE I: Parameters for the PV-Battery buck-boost converter

Parameters	Symbol	Value	Units
Voltage input	$V(\text{in})$	17	V
Voltage output	$V(\text{out})$	13.2	V
Duty cycle	D	44	%
Frequency	f	31.3	kHz
Load	R	3.5	Ω
Minimum Inductor	L(min)	17	μH
Inductor	L	100	μH
Capacitor	C	220	μF
Voltage ripple	$V\Delta$	0.24	V

TABLE II: Parameters for the Battery-Load buck-boost converter

Parameters	Symbol	Value	Units
Voltage input	$V(\text{in})$	13.2	V
Voltage output	$V(\text{out})$	9	V
Duty cycle	D	40	%
Frequency	f	31.3	kHz
Load	R	4.05	Ω
Minimum Inductor	L(min)	23	μH
Inductor	L	100	μH
Capacitor	C	100	μF
Voltage ripple	$V\Delta$	0.288	V

When calculating the duty cycle, it is important to use the absolute value to obtain a positive duty cycle. The load must be calculated according to the supply power with equation (3).

$$P = \frac{(V(\text{out}))^2}{R} \quad (3)$$

Where V is the operational voltage of the load. For the first converter, the voltage $V(\text{out})$ would be the float voltage value of the battery. For the power, it must be considered the energy for the load and the energy to charge the battery. The switching frequency was selected by the isolation elements on/off response times, as well as avoiding the human audible spectrum. With bigger switching frequency, the required inductor and capacitor get smaller. In this case the frequency selected was 31Khz. Finally, voltage ripple is affected by a proper capacitor selection value as in equation(4)

$$\frac{V(\text{out})\Delta}{V(\text{out})} = \frac{D}{RCf} \quad (4)$$

where $V(\text{out})\Delta$ is the voltage ripple desired. As it is the designing parameters are considered at the worst case possible.

The parameters values for the PV-battery buck-boost converter are tabulated in Table(I).

For the Battery-Load buck-boost converter, the design parameters change as the voltage input is now the battery float voltage. As an output voltage, a nominal value of 9V is selected. The parameters for the Battery-Load buck-boost converter are tabulated in Table(II).

When designing, it is important to get duty cycles below 0.5% to have the possibility to enter boost mode. The inductors are also bigger than the minimum to secure continues current in low buck mode.

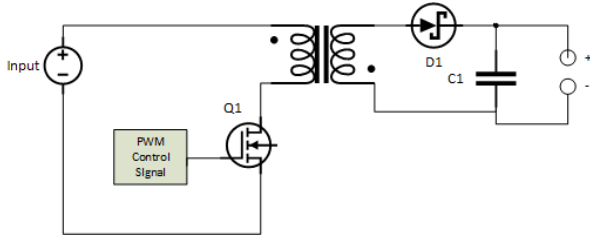


Fig. 3: Flyback converter

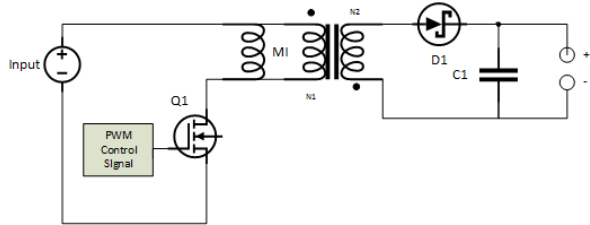


Fig. 4: Equivalent circuit of Flyback converter with magnetizing inductance

B. DC-DC converter with galvanic isolation

The DC-DC converter with galvanic isolation was designed to feed all the instrumentation stage. Due to the low consumption of this stage is possible to use a converter flyback[5] as the one in figure(3).

As in the previous stage the converter needs a continuous current and an acceptable voltage ripple. The challenge in a flyback converter are the use of coupling inductors which gives the inductance required, and a voltage relation between primarily and secondary winding. To dimension the components of the converter we use the equivalent circuit of coupling inductors[5] like in figure (4).

This circuit gives a separated magnetizing inductance and an ideal coupling winding. A similar structure to the previews buck-boost converters can be observed. Equation(5) helps to calculate a minimum magnetizing inductor.

$$L(min) = \frac{(1-D)^2(R)}{2(f)} \left(\frac{N(1)}{N(2)} \right)^2 \quad (5)$$

Where $\frac{N(1)}{N(2)}$ is the turn relation of the windings. For the project, the turn relation is similar to 1 : 1 so the coupling inductor only works as a galvanic isolation device. The problem is that the $L(min)$ calculated is a compound Inductance of the coupling inductors, and just gives an approximated possible value. As a result, the windings must try to have a higher inductance value. Furthermore, it is prudent to have a considerable reactance on the windings to limit the current. This gives a dependence to the *switching frequency* as in equation(6).

$$X(L) = 2\pi fL \quad (6)$$

Since the converter manages low admittance, it can be dismissed to simplified the design. In addition, the correct polarization of the windings is important to the flyback topology and affects directly to the polarization of the Schottky diode. The duty cycle is given by equation(7)

TABLE III: Parameters for the flyback converter

Parameters	Symbol	Value	Units
Voltage input	$V(in)$	13.2	V
Voltage output	$V(out)$	10	V
Min Magnetizing Inductance	$L(min)$	0,2	μH
Turn relation	$\frac{N(1)}{N(2)}$	1:1	
Primarily winding	$L(1)$	87	μH
Secondary winding	$L(2)$	74	μH
Duty cycle	D	43	%
Frequency	f	8.3	kHz
Load	R	33	Ω
Capacitor	C	220	μF
Voltage ripple	$V\Delta$	0.03	V

$$V(out) = V(in) \frac{(D)}{(1-D)} \left(\frac{N(2)}{N(1)} \right) \quad (7)$$

In the secondary winding, the circuit is identical to the buck-boost converter. This equality gives the possibility of determining the load and the voltage ripple with equation(3) and equation(4) respectively. Moreover, the power given to the control and instrumentation stage was designed to be around $2W$. The switching frequency is a crucial point for this converter since it can not be generated by the micro-controller. For this specific converter, a control signal of $21kHz$ is generated by a timer. The control circuit for this converter is exposed in the next section. The parameters for the flyback converter are tabulated in Table(III).

C. Active Components

The three converters previously design have active components that do the switching to step-up or step-down the voltage. The first active component is the diode that lets the circuit supply energy when the mosfet is in off state[7]. Since the switching has a frequency of $31kHz$, the diode must be able to work at high speed and minimize the heat losses. Schottky diodes have a low voltage drop and can work with high speed switching. SB54[8] is a high speed Schottky diode that could manage 3A. The mosfet is the main component of the DC-DC converter. This component works as a high speed switch controlled by a properly control signal. Mosfets usually have heat loses due to the parasitic resistance between drain and source. The IRFB3077[9] power mosfet has a low drain-source resistance of $3.3m\Omega$. By a properly gate-source voltage the resistance goes to $2.8m\Omega$. Since the control stage can not produce a high voltage control signal, the use of a mosfet driver is imminent. When selecting a mosfet driver, it is important to look at the peak current it can supply. Whenever the turn on/off time is smaller, the mosfet pulls more peak current to charge the gate capacitance as in equation(8)

$$I = \frac{Q}{dt} \quad (8)$$

Where Q is the total charge of the mosfet gate and dt is the turn on/off time[10]. The IRFB3077 needs $0.56A$ peak current working with the $31kHz$ control signal. The TC4429[11] mosfet driver manages voltage up to $18V$ and can manage

6A peak current. In addition the TC4429 can be controlled by CMOS/TTL signals.

III. CONTROL STAGE

Control stage specify how the micro-controller implements the Mppt algorithm to the DC-DC converters. It also exposes the implemented control circuits. This section is divided in three topics.

- 1) Control Mppt design
- 2) Instrumentation devices
- 3) Control signals

A. Control Mppt design

A PV can supply an amount of power depending on the solar irradiation[1]. Moreover the load and the battery require constant voltage to work properly. A Mppt algorithm gives a constant voltage or current by tracking the maximum power point for a certain load. This is accomplished by an add and lookout loop. The add and lookout loop calculate and compare the active power at the input and output of the DC-DC converters. If the power input is lower than the output, the micro-controller adds a small value to control signal. However if the power input is higher than the output, it subtract the same small value to the control signal. In addition, it is important to mention that the power depends on the load and the battery charge status. Since the converter tries to keep voltage constant, the current is the one that changes. Figure(5) exposes the action of the designed Mppt algorithm.

Where the limitation parameters are given by the load request and the component limitations. Therefore, this process creates a small oscillation of the control signal. To reduce the consequence of the control signal oscillation in the DC-DC converters, an accurate voltage and current measurement is necessary.

B. Instrumentation devices

The measurement of current and voltage involves conditioning and isolation circuits to let the Analog to Digital Converter (ADC) of the micro-controller work properly[12]. The Atmega micro-controller has a ADC of 10 bits at 5V that gives a resolution of $5 \frac{mV}{bit}$. For current measurement, 20A hall effect sensor will be useful. Since the hall effect sensor does not require any resistive element the energy consume is minimum. Also, it is important to mention that this sensor gives isolation from the power stage. However, the hall effect sensor works with resolution of $100 \frac{mV}{A}$. This means that the current resolution in the micro-controller will be $20 \frac{bits}{A}$. Furthermore, the resolution could be improved with a 5A hall effect sensor but with the restriction of a 5A current top management. For voltage measurement, two circuits are necessary. First, a differential amplifier is used as a conditioning circuit[12]. Figure(6) exposes a differential amplifier with an output given by equation(9).

$$V(out) = \frac{R1}{R2}(V(+) - V(-)) \quad (9)$$

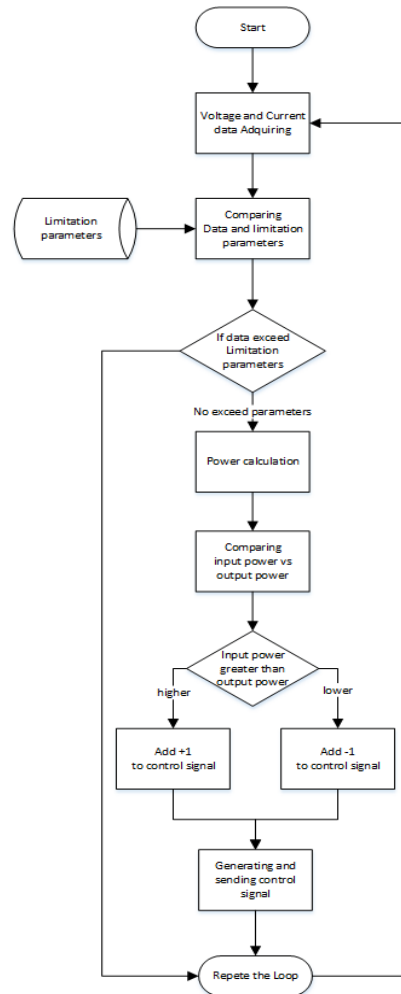


Fig. 5: Flowchart of Mppt algorithm

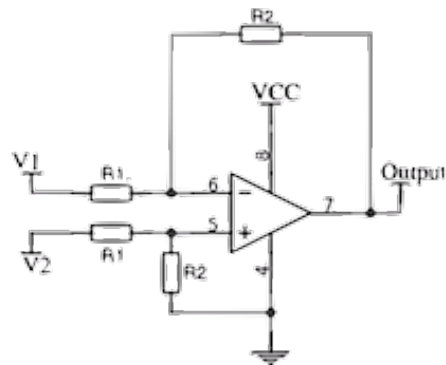


Fig. 6: Differential amplifier

The differential amplifier is connected to the input of the PV and output of each buck-boost converter. When connecting to the buck-boost converters, it is important to remember that the outputs of the converter are inverted by the circuit topology. To acquire the output voltage of the differential amplifier with the micro-controller, it is necessary to isolate the power stage and control stage. Opto-coupler can isolate the two stages but their nonlinearity does not allow an accurate voltage measurement.

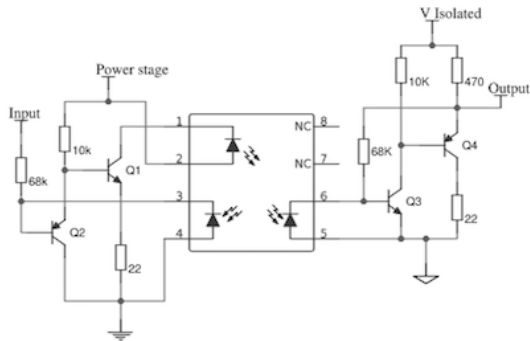


Fig. 7: High speed ultra linear opto-diode circuit

However, opto-diodes gives a great linearity by working with a coupler circuit[13]. Figure(7) exposes a high speed analog isolator using HCNR201[14] as opto-diode with a nonlinearity of 0.01% and a 1 : 1 gain.

Additionally, the isolated circuits need two isolated 5V source. The flyback converter and the battery work as the two isolated voltage source. A LM7805 regulate the voltage to the 5V required.

C. Control Signals

The micro-controller generates the control signals for the buck-boost converters as previously mentioned. The problem is that this signal must be isolated from the power stage as well. Since the control signals work at $31kHz$, the isolation device must be able to switch in less than $15\mu s$. Normal opto-coupler have a response time of $20\mu s$ so the device can not fully saturate the transistor and the control signal get deformed. As a solution a device with a smaller response time must be used. The opto-nand 6N137[15] has a response time of $48ns$ and also gives clean CMOS signal due to the integrated Nand gate. The output of the opto-nand goes to the mosfet gate-drive of the power stage.

The isolation devices are powered by the flyback converter. This means the flyback converter needs to be powered directly by the battery to always supply energy to the control stage. The control signal for this converter is generated by a LM555[16] Timer as in figure(8).

The control signal is designed using the following equations(10).

$$f = \frac{1}{(R1 + 2R2)C1} \quad (10)$$

$$D = \frac{R1}{R1 + R2}$$

The used diodes help the timer to generate a Duty cycle higher than 0.5%. The parameters value for this circuit are tabulated in Table(IV)

Even though the timer circuit is part of the control stage of the flyback converter, it is the only control circuit that is directly connected to the power stage.

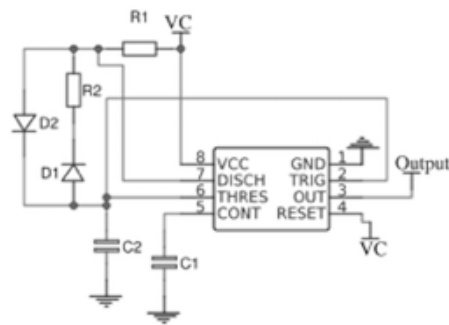


Fig. 8: 555 Timer PWM generator circuit

TABLE IV: 555 Timer Parameters for control signal

Parameter	Symbol	Value	units
Voltage amplitude	Vpp	12	V
Frequency	f	8.3	kHz
Duty cycle	D	28	%
Resistance 1	R1	2	k Ω
Resistance 2	R2	5	k Ω
Capacitance 1	C1	10	nF
Capacitance 2	C2	10	nF

IV. RESULTS

The implementation of the circuits was made on a PBC using the software Altium Design. For protection purpose, fuse and peak suppressor diodes were included in the design. The solar charger controller, as shown in Figure(9)

has been implemented and tested with an 10 ohms resistor as load. For such a test, the load voltage has been set up on $7.7Volts$. The solar charger controller test consists on supplying energy to the load for a considerable amount of time $2hours$. During the test time, the PV was covered so the solar irradiation change and the voltage dropped down. Here the

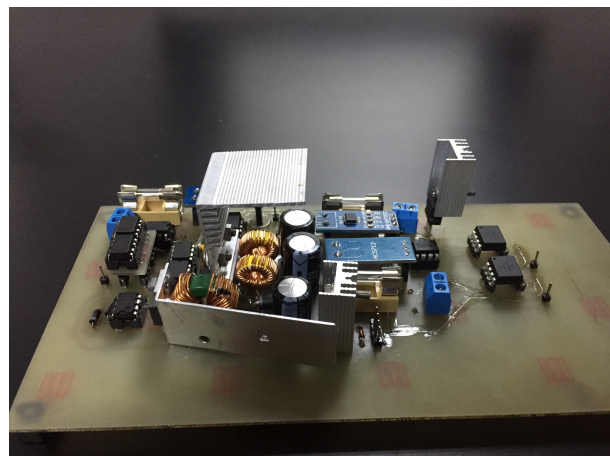


Fig. 9: Implemented solar charger controller

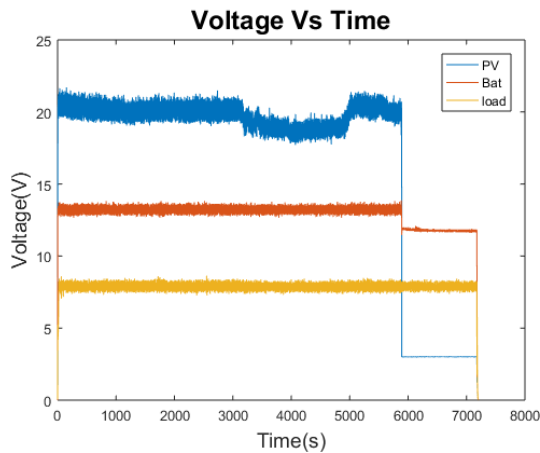


Fig. 10: Voltage Wave form

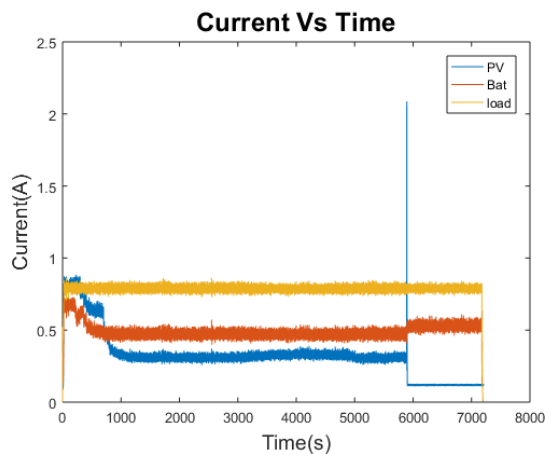


Fig. 11: Current wave form

battery needed to supply energy to the load. Using the micro-controller as a data acquisition(DAQ) it was possible to get the following plots.

The Voltage Vs Time plot(10) show the voltage of the PV, Battery and the load. Even though the Voltage present a considerable oscillation, the mean voltage of the load is almost constant. The battery mean voltage is also constant until the point where the PV Voltage drops. The battery began to supply energy to the load without problem keeping load voltage constant. As mentioned previously, the PV voltage depends on the solar irradiation and the PV voltage plot display the lack of irradiation due to some clouds. The Current VS Time plot(11) display the current at the input of the PV, the current at the output of the first buck-boost converter, and the current supplied to the load. As it can be seen, the current plot is inverted respect to the voltage plot. This is because the converters work on buck mode so the power transformation require an increase on the current. It is importance to analyze the beginning of the plot where the battery and the load pull energy from the PV. This goes on until the battery charge and stay on the float mode. The next transient occurs when the PV voltage drop down. As the voltage drops the buck-boost converter tries to compensate by increasing the current. Since voltage goes down 5V the control shutdown the PV-Battery

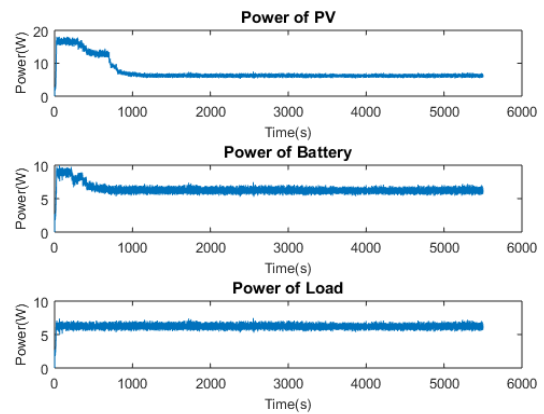


Fig. 12: Active Power

TABLE V: Mean of acquired data

Parameter	Symbol	Mean	Units
Voltage PV	V(PV)	16.7578	V
Voltage Battery	V(Bat)	12.9131	V
Voltage Load	V(Load)	7.8466	V
Current PV	C(PV)	0.3206	A
Current Battery	C(Bat)	0.4881	A
Current Load	C(Load)	0.7847	A
Power PV	P(PV)	7.3498	W
Power Battery	P(Bat)	6.3703	W
Power Load	P(Load)	6.1998	W

converter and only a current peak is shown on the plot.

To finalize the section, the active power is calculated and displayed on Figure(12)

Since the plots present oscillation the mean of the data were tabulated in Table(V). The mean must be estimated before the PV voltage goes down to have accurate mean calculation.

The calculated means gives a Power efficiency of 86,67% between the PV and the Battery and a efficiency of 97,32% between the Battery and the Load.

V. CONCLUSION

In this paper, a solar charger controller is presented. The proposed electronic device could manage the energy of a 100W solar panel and supply energy to any kind of load. Regardless the battery charging time, the efficiency of the DC-DC power converters could reach 97% but if the case warrants the device could charge and supply energy to a load with a efficiency higher than 84%. Since the Load Voltage could easily be set up without the need to recalculate the electrical component values, the proposed device could be applied in several energy management project that use solar energy.

REFERENCES

- [1] M. Sheraz, G. A. Akhtar, and M. Abido, "Intelligent controller to extract maximum power from solar park."
- [2] U. Kamnarn, S. Yousawat, S. Sreeta, W. Muangjai, and T. Somsak, "Design and implementation of a distributed solar controller using modular buck converter with maximum power point tracking," in *Universities Power Engineering Conference (UPEC), 2010 45th International*. IEEE, 2010, pp. 1–6.

- [3] K. Ananda-Rao, R. Ali, S. Tanisclass, and N. H. Baharudin, "Micro-controller based battery controller for peak shaving integrated with solar photovoltaic," 2016.
- [4] SunLink, "High efficiency mono-crystalline solar module," Tech. Rep. [Online]. Available: <http://www.sunlink-energy.com/UploadFiles/2012/281/2012112601482188668.pdf>
- [5] D. W. Hart, *Power Electronics*. Pearson Education, 2011.
- [6] C. L. Espinosa, "Asynchronous non-inverter buck-boost dc to dc converter for battery charging in a solar mppt system," in *URUCON, 2017 IEEE*. IEEE, 2017, pp. 1–4.
- [7] A. Sarikhani, B. Allahverdinejad, and H. Torkaman, "A non-isolated buck-boost dc-dc converter with single switch," in *Power Electronics, Drives Systems and Technologies Conference (PEDSTC), 2018 9th Annual*. IEEE, 2018, pp. 369–373.
- [8] Vishay, "Schottky barrier plastic rectifier," Tech. Rep. [Online]. Available: <https://www.vishay.com/docs/88719/sb320.pdf>
- [9] I. Rectifier, "Hexfet power mosfet," Tech. Rep. [Online]. Available: <https://www.infineon.com/dgdl/irfb3077pbf.pdf>
- [10] J. Dunn, "Matching mosfet drivers to mosfets," *Microchip Technology Inc*, pp. 4–5, 2004.
- [11] Microchip, "6a high-speed mosfet drivers," Tech. Rep. [Online]. Available: <http://ww1.microchip.com/downloads/en/DeviceDoc/21419D.pdf>
- [12] D. Placko, *Fundamentals of instrumentation and measurement*. John Wiley & Sons, 2013.
- [13] Y.-q. TAN, D.-p. FAN, and Y. TAO, "Design and implementation of dsp acquisition circuit based on linear optocoupler hcnr200 [j]," *Electrical Measurement & Instrumentation*, vol. 6, p. 012, 2006.
- [14] A. Tecnologies, "High-linearity analog optocouplers," Tech. Rep. [Online]. Available: <https://www.edn.com/Pdf/ViewPdf?contentItemId=4127132>
- [15] Vishay, "High speed optocoupler, single and dual, 10 mbd," Tech. Rep. [Online]. Available: <https://www.vishay.com/docs/84732/6n137.pdf>
- [16] T. Instrument, "Lm555 timer," Tech. Rep. [Online]. Available: <http://www.ti.com/lit/ds/symlink/lm555.pdf>